JOURNAL OF CATALYSIS **159,** 178–188 (1996)
ARTICLE NO. 0077

Characterization of Bimetallic Pt–Sn/Al_2O_3 Catalysts: Relationship between Particle Size and Structure

E. Merlen,* P. Beccat,* J. C. Bertolini,† P. Delichère,† N. Zanier,* and B. Didillon*,[1]

*Institut Français du Pétrole, 1&4 av. de Bois Préau, BP311, 92506 Rueil-Malmaison, France; and
†Institut de Recherche sur la Catalyse, 2 av. Albert Einstein, 69626 Villeurbanne, France

Received April 3, 1995; revised October 13, 1995; accepted November 1, 1995

Pt–Sn/Al_2O_3 bimetallic catalysts have been prepared using organometallic precursors and characterized. Two models depending on average platinum particle size are proposed in order to describe these solids. The catalyst obtained from a highly dispersed monometallic precursor may be described as Pt/SnO_x/Al_2O_3 with platinum probably in interaction with tin oxide. When the monometallic precursor has low dispersion, the bimetallic system may be described as $PtSn^0$ + SnO_x/Al_2O_3.

1. INTRODUCTION

Alumina supported platinum–tin catalysts are of major importance in refining and petrochemistry. Tin addition is now well known to increase the selectivity of such catalysts toward aromatics in naphtha reforming. This system is also used, for example, in the dehydrogenation of isobutane. However, the effect of tin is not clearly understood today.

Although few papers are dedicated to a comparison of the physicochemical and catalytic properties of such systems (1–3), it seems that the preparation technique is of great importance in determining these properties. Alumina supported platinum–tin systems may be obtained using the sol–gel technique (4), impregnation, and solvated metal atom dispersion (SMAD) (5–7), as well as by surface organometallic chemistry (8, 9).

From a structural point of view, most studies are related to model samples. Surface alloy phases such as Pt_3Sn or Pt_2Sn have been obtained by tin vapor deposition on Pt (111) monocrystals followed by annealing treatments (10). The PtSn alloy has been obtained in the same way for a (100) Pt orientation (11). Some studies have been devoted to model catalysts for which either particles or supports are considered as models. The former are generated by coevaporation of platinum and tin or by SMAD, and very small and/or amorphous Pt–Sn particles have been detected (6). A microstructural study of Pt–Sn particles on amorphous silica (12) may be given as an example of the use of model supports. After H_2 treatment, intermetallic compounds are formed and, after oxidation, particles are described as platinum crystallites decorated by small SnO_2 crystals both in contact with SiO_2. In the case of practical catalysts, alloy formations (PtSn, Pt_2Sn, and $PtSn_2$) have been observed after thermal treatment on spinel oxide supports $ZnAl_2O_4$ and $MgAl_2O_4$ (13). For alumina or silica supports, results depend on the preparation technique used. When the metals are introduced together by use of a bimetallic complex $(Pt_3Sn_8Cl_{20})^{2-}$ (14) or by coimpregnation of H_2PtCl_6 and $SnCl_4$ (15, 16), the PtSn alloy (14, 15) or bimetallic particles (14) are formed. However, for a similar preparation neither metallic tin nor alloy formation was detected by other authors (17). For platinum deposited on a tin–alumina coprecipitate, microdiffraction patterns have been interpreted as Pt–Sn alloy patterns, but only platinum was detected on the majority of particles, and XRD (X-ray diffraction) showed no evidence of alloy formation (15). EXAFS (extended X-ray absorption fine structure) data on the same type of samples led to the conclusion that platinum particles were on the support surface containing Sn^{2+} ions (16).

The oxidation states of tin and platinum are also of great interest. Work on the reducibility of oxidized catalysts has mainly focused on Pt–Sn particles supported on chlorine doped alumina. It has been established that interaction between platinum and tin is obtained using coimpregnation (2, 3) and by calcination at a temperature higher than 500°C when successive impregnations are used (9). It has also been established that reduction of tin is favored in the presence of platinum (9). Hydrogen consumption has shown that both metals are never totally reduced. Thus the alloy phase is never formed alone. However, many different results have been reported, probably because of different preparation techniques and different treatments.

In reduced bimetallic systems obtained by nonconventional methods (SMAD) (5, 6) and using an organometallic precursor for preparation (18), both Pt and Sn are metallic. When more conventional preparation techniques are used, Sn^{IV}, detected by Mössbauer spectroscopy, is always present on catalysts even after reduction at 500°C. The

[1] To whom correspondence should be addressed.

0021-9517/96 $18.00

Sn^{IV}/Sn_{total} ratio depends on the type of support (19), the Sn/Pt ratio (20), the metal and chlorine loadings (21), and the particle size (22). The exact nature of the phase containing Sn^{IV} is still a subject of discussion. Sn^{II} was also seen by Mössbauer spectroscopy and its percentage is related to the type of support. For a given support, discrepancies in reported results indicate that conditions of preparation and of observation have to be taken into account. Finally, many studies focused on the detection of metallic tin, and again results vary widely on this subject. In some cases, no metallic tin has been found (19, 23, 24). If it is present, its percentage is related to the presence of chlorine (24), preparation, specific area (25, 26), metal loadings (21), Sn/Pt ratios, and supports. Metallic tin is present either in Pt–Sn alloys or as isolated metallic tin.

Thus, the role of tin and its oxidation state in alumina supported Pt–Sn catalysts after activation treatments have been extensively reported. However, the oxidation state of tin, the different platinum tin phases, and the electronic modification of platinum by tin are still subjects of discussion. They seem to depend on the Pt/Sn ratio, methods used to prepare catalysts, including precursors and the type of impregnation, and metallic particle sizes. The aim of the present work is to attempt to elucidate the sate and the role of tin in alumina supported platinum–tin catalysts. For this, monometallic platinum and bimetallic catalysts were prepared using organometallic precursors. According to previous studies, "well defined catalysts" may be obtained by this technique. We have focused our study on the influence of tin loading and of particle size on the structure of bimetallic catalysts and on the electronic effect of tin on platinum. Catalysts have been described in terms of dispersion, surface composition, oxidation state, and electronic interactions. For the latter, we used a variety of investigation techniques, described in the literature, to determine the amount of electronic transfer between metals in bimetallic systems such as infrared studies of adsorbed carbon monoxide, orthoxylene hydrogenation, and already published XANES (X-ray absorption near edge structure) experiments. This study made a comparison of results from these techniques to evaluate their ability to determine the "electronic effect" in bimetallic catalysts.

2. EXPERIMENTAL

Preparation of catalysts. The support used was a γ alumina with a surface area of 200 m^2/g and a pore volume of 0.6 cm^3/g. Before use, the support was calcined for 2 h at 530°C in air. A highly dispersed monometallic catalyst (M1) was obtained by excess impregnation of the alumina using platinum bisacetylacetonate in toluene (using a solvent to support mass ratio of 5 and a complex to competitor (acetylacetone) ratio of 0.2). The impregnation was carried out at room temperature under steady-state conditions for 72 h. After filtration, the catalyst was dried for 12 h at 120°C, calcined for 2 h at 530°C in an air stream, and then reduced under hydrogen at 450°C. In order to obtain lower dispersions (samples M2, M3, and M4), the reload technique (27) was employed. Here platinum bisacetylacetonate was decomposed under hydrogen on the reduced monometallic catalyst. The presence of a competitor (acetylacetone) favored the decomposition of the complex on the metal rather than on the support. The catalysts were then filtered, calcined at 350°C, and reduced at 450°C.

TABLE 1

Characteristics of the Catalysts and Chemisorption Results

Samples	Pt wt%	Sn wt%	Dispersion by titration (%)	H_2/Pt
Sn	0.00	0.23		0.00
M1	0.68	0.00	87	0.52
B11	0.68	0.38		0.31
B12	0.69	0.62		0.23
B13	0.69	0.82		0.22
M2	2.06	0.00	63	0.35
B21	2.10	1.05		0.18
B22	2.10	1.44		0.13
B23	2.10	1.53		
M3	2.40	0.00	51	0.28
M4	3.30	0.00	32	0.29
B41	3.26	0.44		0.24
B42	3.28	1.16		0.14
B43	3.39	1.32		0.14

Bimetallic catalysts were prepared from Pt/Al_2O_3 monometallic catalysts. After a reduction at 450°C for 2 h under hydrogen, the sample was transferred under nitrogen in a reactor filled with *n*-heptane. After hydrogen purge for 1 h at 80°C, a quantity of tetrabutyl tin was introduced in order to obtain the Pt/Sn ratio desired. After impregnation at 80°C (until C_4 compounds were no longer produced), the catalyst was washed with *n*-heptane, dried for 12 h at 120°C, and reduced at 450°C. Bimetallic samples are denoted "B*mn*" where *n* corresponds to the reference of the monometallic catalyst used for their preparation and *m* to the order of increasing tin content.

A monometallic catalyst, referred to as Sn, containing 0.23 wt% of tin was also prepared following similar preparation techniques.

The characteristics of all the solids are given in Table 1.

Chemisorption. Experiments were performed using a χSorb apparatus. Catalysts were reduced at 500°C. After quenching under hydrogen at room temperature, the adsorption of hydrogen was measured. A stoichiometry of one atom of hydrogen per atom of Pt was used to determine the accessibility of platinum. For the monometallic catalysts, chemisorbed hydrogen was titrated by oxygen.

This last measurement gives the dispersion of the metallic phase.

Transmission electron microscopy (TEM). TEM was carried out on a JEOL 2010 at 200 kV. Samples were crushed in ethanol and deposited on a copper grid coated with a perforated carbon film. A VG HB5 scanning transmission electron microscope (STEM) (100 kV) equipped with a TRACOR TN524 X-ray energy dispersive spectrometer (X-EDS) was used for local analysis.

Temperature programmed reduction (TPR). TPR was performed on a χSorb apparatus with 5% H_2 in Ar. Samples were calcined at 530°C before reduction, and the heating ramp was 5°C/min.

X-ray photoelectron spectroscopy (XPS) and low-energy ion scattering (LEIS). Experiments were performed in an ESCALAB 200R system from Fisons Instruments, with a base pressure lower than 3×10^{-10} mbar. Catalysts were studied both after calcination and after reduction. Reduced catalysts were transferred under hydrogen from the reactor to the vacuum chamber. XPS analysis was performed using the Mg source on the dual anode source. The pass energy of the hemispherical electron analyzer was 50 eV, and the collection angle of the photoelectrons with respect to the plane of the surface was 90°. XPS measurements provided quantification of the surface Pt/Sn ratios and a study of the oxidation state of tin. Determination of the oxidation state of platinum is difficult as the Pt 4*f* signal is superimposed with that of aluminum, and the Pt 4*d* signal was too noisy to be used for this determination. The Pt 4*d* signal was used for quantification only. Reduction conditions were as follows: 5°C/min, $T_{max} = 500$°C for 2 h, $H_2 = 12$ liter/h. LEIS measurements were performed with 1 keV He^+ ions at a scattering angle of 150°. The intensity of the primary beam was fixed at 20 nA into an impact spot of around 1 mm diameter. In these experimental conditions, we determined the LEIS relative sensitivity factors of Sn and Pt by analyzing a $Pt_3Sn(111)$ face lent by Bardi and colleagues and for which they found that the first atomic layer has the same composition as the bulk (28).

Infrared spectroscopy coupled with CO chemisorption (IR(CO)). IR(CO) was carried out by a DIGILAB FTS80 interferometer. The sample (20 mg) was pressed under 200 kg/cm^2 and placed in an *in situ* cell. The disk diameter was 16 mm. A pretreatment was applied in the following conditions: heating to 450°C (5°C/min) under a secondary vacuum (3.7×10^{-6} Torr), then reduction under hydrogen for 4 h, and finally 12 h under a vacuum. Carbon monoxyde (1 vol% in Ar) was introduced at 25°C by pulses until both the integrated surface and wavenumber of the vibration band of linear CO adsorbed on Pt atoms were stabilized. A dispersion of CO was obtained by heating the sample to 150°C during 15 min under CO pressure. The sample was then heated under secondary vacuum at 25°C for 1 h and then from 80°C during 30 min by steps of 20°C until total CO desorption was obtained. After each step, spectra were obtained at room temperature in transmission mode with an accumulation time of 100 s and a resolution of 4 cm^{-1}.

Catalytic tests. Hydrogenation of orthoxylene was chosen as a test reaction in order to detect differences in electronic density of the metals. The *cis*-dimethylcyclohexane is favored by a high electron density on platinum (29). A quartz reactor with a volume of 80 cm^3 and a diameter of 2.5 cm was used. Orthoxylene (Aldrich) and hydrogen (Air Liquide) were dried before use. Samples were reduced at 450°C under hydrogen (6 liter/h) before catalytic tests. The reaction conditions were as follows: 0.2 to 1 g of catalyst, 150°C, 6 liter/h of hydrogen, and 6 to 50 ml/h of orthoxylene. Quantity of catalyst and orthoxylene flow were adjusted in order to maintain less than 10% conversion.

3. RESULTS

Catalyst Dispersion

Dispersion values for the monometallic Pt/Al_2O_3 catalysts were determined by H_2–O_2 titration. The results are presented in Table 1. It can be seen that a range of dispersions was obtained. The corresponding particle sizes can be calculated using a structural hypothesis (cubic, bipyramidal, and cuboctahedral). Values obtained are 1.0, 1.8, 2.3, and 4.0 nm, respectively, for M1, M2, M3, and M4 whatever the model used. As shown in Fig. 1, good correlation is obtained between these dispersions and hydrogen chemisorption. Hydrogen chemisorption measurements were therefore used to describe platinum accessibility of bimetallic catalysts (see Table 1). It is immediately clear that addition of tin decreases the accessibility of platinum.

Average sizes of particles were also evaluated by direct observation by TEM. A typical micrograph is shown in Fig. 2 with the corresponding histogram established from measurements of about 300 particles. Results obtained by

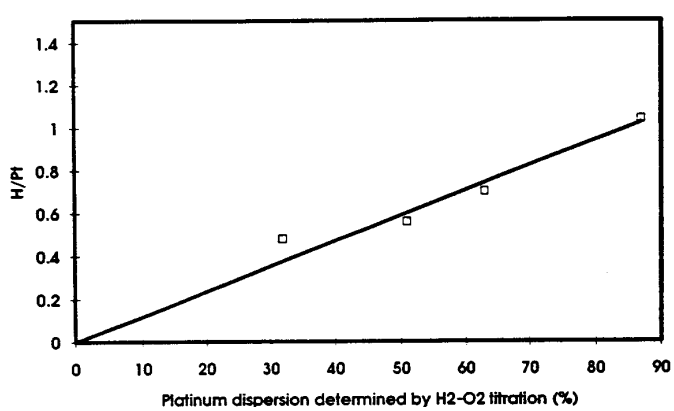

FIG. 1. Correlation between dispersion and quantity of chemisorbed hydrogen.

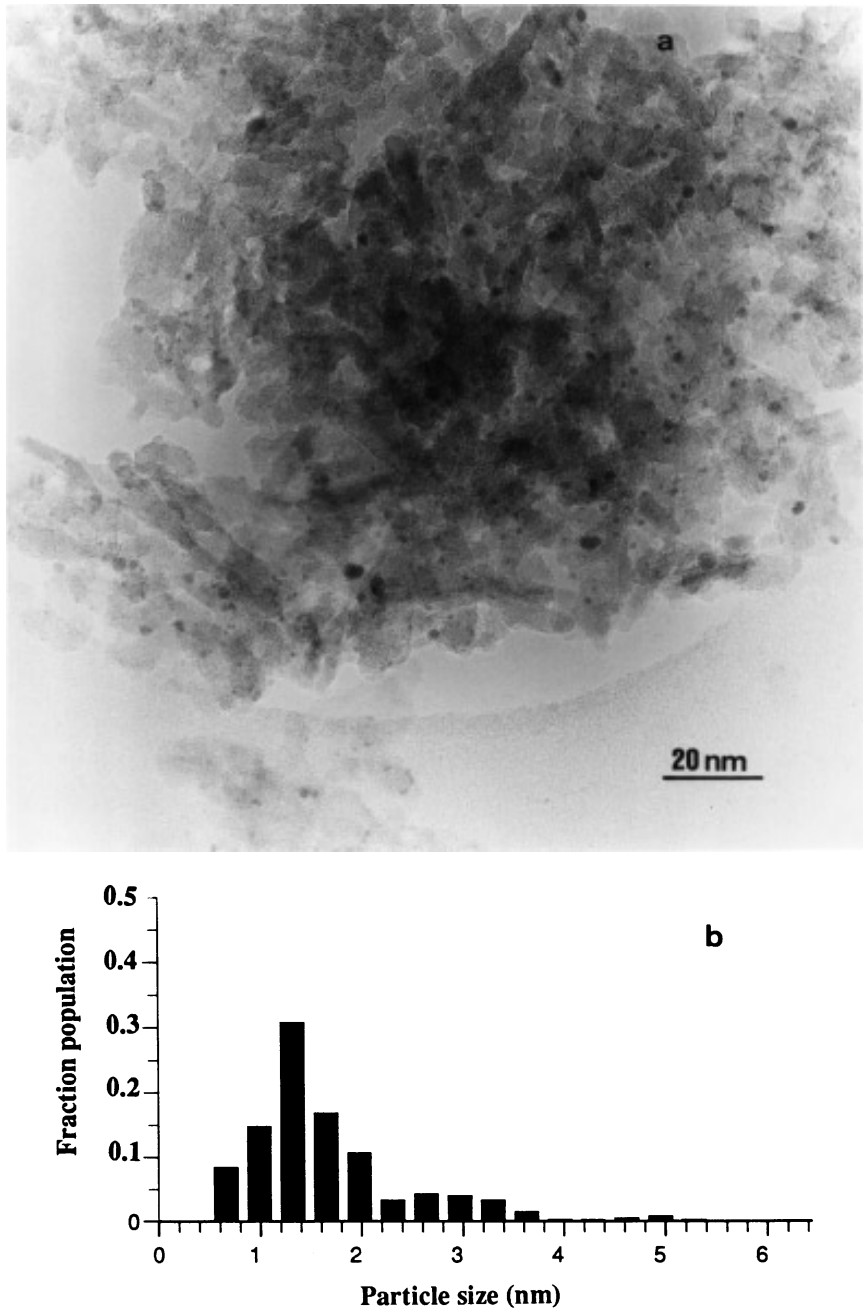

FIG. 2. (a) Typical micrograph obtained for sample M2. (b) Histogram of the sample.

TEM are summarized in Table 2. The average size and the size of highest frequency both shift to higher values as the platinum loading is increased (M1, M2, and M4).

When tin is added, the evolution of particle size due to tin additives depends on the average particle size of the corresponding monometallic precursor. For the highest (M1) and the smallest (M4) initial dispersion, no evolution can be detected. An increase in the size of highest frequency with an increase in the amount of tin is observed, however, for intermediate dispersion (M2 precursor).

Surface and Particle Chemical Composition

Quantitative results obtained by XPS for calcined and reduced samples are presented in Table 3. The following remarks can be made taking into account the relative accuracy of this technique (about 20%). First, it seems that reduction does not influence the amounts of Pt and Sn detected. Second, Pt/Sn ratios obtained by XPS are always lower than bulk values established by X-ray fluorescence (Fig. 3). As the depth analyzed by XPS in 4 nm, and considering average particle sizes, only a heterogeneous distribution of Pt and

TABLE 2

Particle Distributions Obtained from TEM Measurements

Sample	Histogram limits (nm) (min/max)	Size of highest frequency
M1	0.7/2.0	1.0
B11	0.7/2.3	1.0–1.3
B12	0.7/2.3	1.0–1.3
B13	0.7/2.3	1.0
M2	0.7/5.3	1.3
B21	0.7/9.6	1.3–1.6
B22	0.7/5.6	1.6
B23	0.7/6.9	2.0
M4	1.0/5.9	2.0
B41	1.0/6.3	1.6–2.0
B42	0.7/7.3	2.0–2.3
B43	0.7/6.3	2.0–2.3

Sn can explain the result. Tin may for instance be present as a dispersed phase with the particles mainly containing platinum.

LEIS results are presented in Table 4 for calcined and reduced samples. Spectra of B42 catalyst (reduced or oxydized) are presented on Fig. 4. For all catalysts, a first spectrum was acquired in 50 s on the nonmodified surface: this analysis is considered to be at time $t = 0$ s. The surface being eroded by incident He^+ ions, spectra at $t = 10$ min and $t = 30$ min were acquired in order to give a qualitative description of the profile of concentrations. Relative atomic percentages of tin (Sn + Pt = 100%) are very high, from 70 to close to 100, indicating that the first layer is tin-rich. Tin enrichement is generally decreased by reduction. In addition, under this first layer, the study of the profiles shows that platinum atomic percentage increases. This evolution is less pronounced for reduced samples than for calcined samples. This would indicate that, after reduction, catalysts are more homogeneous in depth.

Additional information was obtained by the study of the local composition of sample B43 by STEM. Pt/Sn ratios

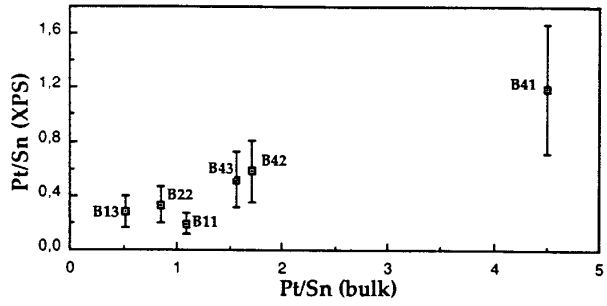

FIG. 3. Pt/Sn ratios determined by XPS as a function of Pt/Sn bulk ratios.

of particles and of areas of support were determined. Note that the different particle sizes are not representative to the average sample. We have chosen particles in a wide range of sizes to determine the effect of particle size on particle composition. Pt/Sn atomic ratios obtained for the support were always lower than the nominal value of 1.56 and close to 1. Moreover, it was possible to establish that, for particles, the Pt/Sn atomic ratio was always greater than the nominal value and increased with particle size (Fig. 5). Here, the signals detected from the particles were corrected for the contribution due to the support. Although the correction is not exact due to local heterogeneity of the support composition, the resulting evolution of Pt/Sn atomic ratio versus particle size is clear.

Oxidation State

The Sn $3d_{5/2}$ peak obtained by XPS contains two contributions. The first is Sn^0 with a binding energy of 484.6 eV and the second is Sn^{II} and/or Sn^{IV} which cannot be separated as their binding energies are too close (486.6 and 486.4 eV, respectively). The monometallic sample Sn was calcined and used as a totally oxidized standard for these measurements and gave in this case 15% Sn^0 and 85% tin oxides. This result is probably due to the background subtraction and is considered as the limit of detection of metallic tin for the decomposition technique used. Results obtained for

TABLE 3

Quantitative XPS Analysis after Calcination (Calc.) and Reduction (Red.).

	Al 2*p*		O 1*s*		C 1*s*		Sn 3*d*		Pt 4*d*	
Samples	Calc.	Red.	Calc.	Red.	Calc.	Red.	Calc.	Red.	Calc.	Red.
B11	43	43	55	56	1.4	0.0	0.26	0.27	0.06	0.05
B13	39	39	57	60	3.0	5.7	0.37	0.40	0.08	0.11
B21	44		51		4.6		0.42		0.13	
B22	43	46	48	53	8.5	0.0	0.50	0.43	0.15	0.14
B41	46	47	51	52	2.3	0.0	0.27	0.26	0.24	0.31
B42	46	47	51	51	1.9	1.1	0.44	0.38	0.24	0.22
B43	47	47	51	51	1.9	1.1	0.48	0.42	0.22	0.22

Note. Results are given in at.% with a relative error estimated as 20%.

TABLE 4

Quantitative LEIS Analysis after Calcination (Calc.) and Reduction (Red.) in Relative at.%

	$t = 0$ min				$t = 10$ min				$t = 30$ min			
	Pt		Sn		Pt		Sn		Pt		Sn	
Catalysts	Calc.	Red.	Calc.	Red.	Calc.	Red.	Calc.	Red.	Calc.	Red.	Calc.	Red.
B11	10	15	90	85	23	18	77	82	29	22	71	78
B13	8	7	92	93								
B21	9	11	91	89	24	21	76	79				
B22	5	15	95	85	16	15	84	85				
B41	18	29	82	71	43	29	57	71	56	38	44	62
B42	9	15	91	85	21	21	79	79	38	25	62	75
B43	15	16	85	84	22	25	78	75	27	29	73	71

the catalysts after calcination and after reduction are presented in Table 5. Sn^0 is clearly present after calcination. Moreover, although the percentage of Sn^0 increases after reduction, a part of oxide tin cannot be reduced. This is clearly shown in Fig. 6 which presents Sn $3d5_2$ decomposition for the sample B42 before the after reduction. Finally, particle size seems to influence the reducibility of tin. Indeed, reduction hardly changes the state of tin for samples B11 and B13 but has a great effect for series B4. In addition, in this latter case, the fraction of Sn^0 increases with the tin loading.

TPR data can be used to determine the quantity of hydrogen required to reduce the sample and the temperature of maximum consumption of H_2. The results are presented in Table 6. TPR profiles of monometallic percursors M1, M2, and M4 are shown in Fig. 7a and those of samples M4, B41, and B42 in Fig. 7b. When the average size of the particles increases, the amount of hydrogen consumed per platinum atom decreases. This nonstoichiometric reduction results from the fact that the larger particles are more difficult to reoxidize totally in the calcination preceeding TPR measurements. The reduction temperatures also vary with average particle sizes. It is worth noting

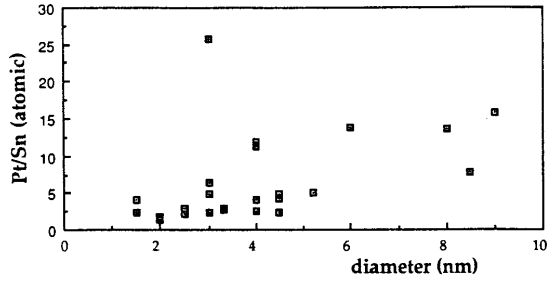

FIG. 5. Evolution of Pt/Sn atomic ratio with particle diameter determined by XEDS.

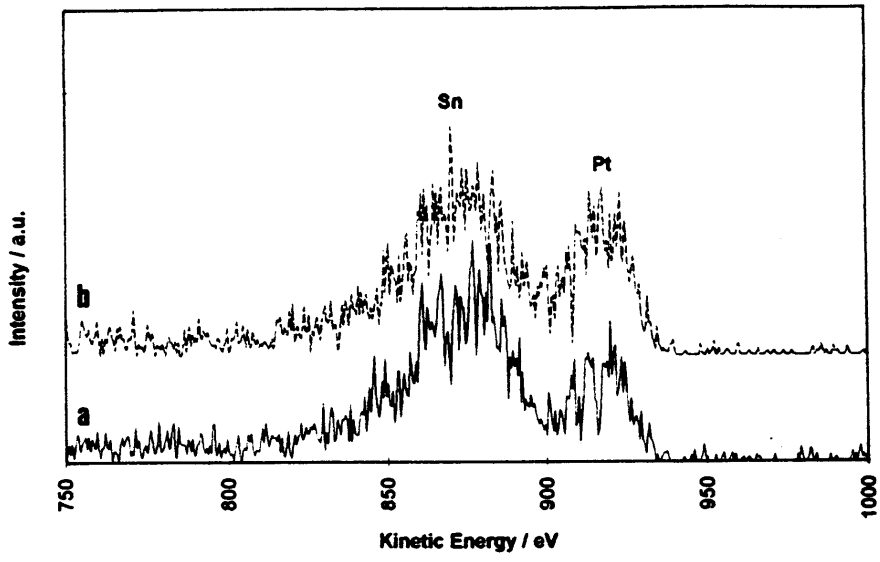

FIG. 4. LEIS spectra of sample B42 (analysis at time = 0 s) (a) before reduction and b) after reduction.

TABLE 5

Relative Percentages of Metallic and Oxide Tin Obtained by Decomposition of the Sn $3d_{5/2}$ signal

	After calcination		After reduction	
Catalysts	Metallic Sn	Oxidized Sn	Metallic Sn	Oxidized Sn
B11	27	73	28	72
B13	37	63	33	67
B21	18	82		
B22	20	80	35	65
B41	27	73	41	59
B42	18	82	55	45
B43	22	78	63	37

TABLE 6

TPR Results

	wt.%		Reduction temperatures		
Catalysts	Pt	Sn	(°C)[a]	VH_2 (cm^3/g)	H_2Pt
Sn		0.23	220–400	0.35	0.76[b]
M1	0.68		290–175–100 (s)[c]	2.21	2.64
B11	0.69	0.38	150 (vl)[d]–275–425	1.40	1.67
B13	0.69	0.82	100–120	2.29	2.73
M2	2.06		300–75–175	3.36	1.32
B21	2.10	1.05	100	2.25	0.89
B22	2.10	1.44	100–175 (s)–450 (s)	3.51	0.93
M3	2.40		325–75	2.31	0.78
M4	3.30		325–60	2.49	0.61
B41	3.26	0.44	65–360–180(s)	2.93	0.72
B42	3.28	1.16	75	2.02	0.50

[a] Temperatures are given in order of decreasing peak intensity.
[b] H_2/Sn ratio.
[c] Shoulder.
[d] Very large.

that two types of Pt oxides are considered in the literature, one in weak interaction with the support and the other in strong interaction (30). The former may be reduced at low temperatures (<100°C), and the latter requires high temperatures (300°C). For the highly dispersed monometallic catalyst M1, the peak of largest area is at 290°C. A second peak at lower temperature with a relative intensity which increases with particle size is present (samples M2 and M4, Fig. 7a). In the reduction of bimetallic systems, hydrogen consumption is lower than that needed for the reduction of Pt^{IV} to Pt^0 and Sn^{IV} to Sn^{II} seen in the corresponding monometallic systems. Either one phase (alloy-type?) is not reoxidized and thus remains in a metallic form, or an oxide phase is not reduced during the TPR. XANES data have shown that platinum is fully reduced after H_2 treatment (31). Thus the first hypothesis will be retained. On adding tin to platinum supported catalysts, the area of the high temperature peak decreases and the low temperature peak increases as if tin could isolate particles from the support. The reduction peak of oxide tin is not visible, indicating that no independent tin is present on the support.

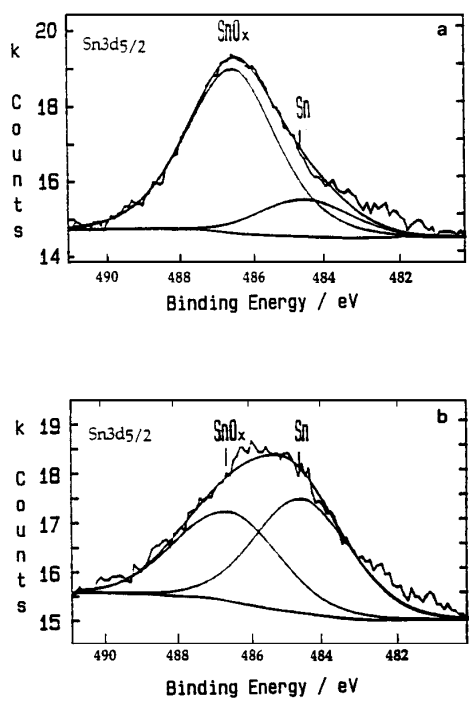

FIG. 6. Decomposition of the Sn 3*d* 5/2 signal in Sn metal and Sn oxide for sample B42 (a) before reduction and (b) after reduction.

Electronic Effects

Infrared spectroscopy coupled with CO chemisorption allows the study of electronic effects through the frequency shift of the stretching vibration of CO adsorbed on a platinum atom. To avoid dipole–dipole interactions, ν_{C-O} frequencies were measured for CO surface coverage close to zero evaluated by extrapolation. This was obtained by thermodesorption of previously adsorbed CO. For the series M1, B11, and B12, addition of tin results in a shift referred to M1 of $+6\ cm^{-1}$ (from 2033 to 2039 cm^{-1}) interpreted as a decrease in electronic density of the platinum atoms. No shift was detected for series 2 with frequencies of 2037–2038 cm^{-1} or for series 4 with frequencies of 2040–2041 cm^{-1}.

Orthoxylene hydrogenation has been described as a reaction capable of measuring electronic interactions in bimetallic catalysts (29). The reproducibility of orthoxylene tests was first determined. To avoid any isomerization of reaction products, the conversion rate had to be as low as possible and at least below 10%. Conversion and selectivity values are given with an accuracy of 5%. After this operating time, for all catalysts, selectivities and activities no longer varied. It was checked that the reaction was not diffusion limited by determining an apparent activation energy of 12.1 kcal/mol in agreement with previous data (32).

Activities of the catalysts were determined, and TOF data (molecules of orthoxylene transformed per surface

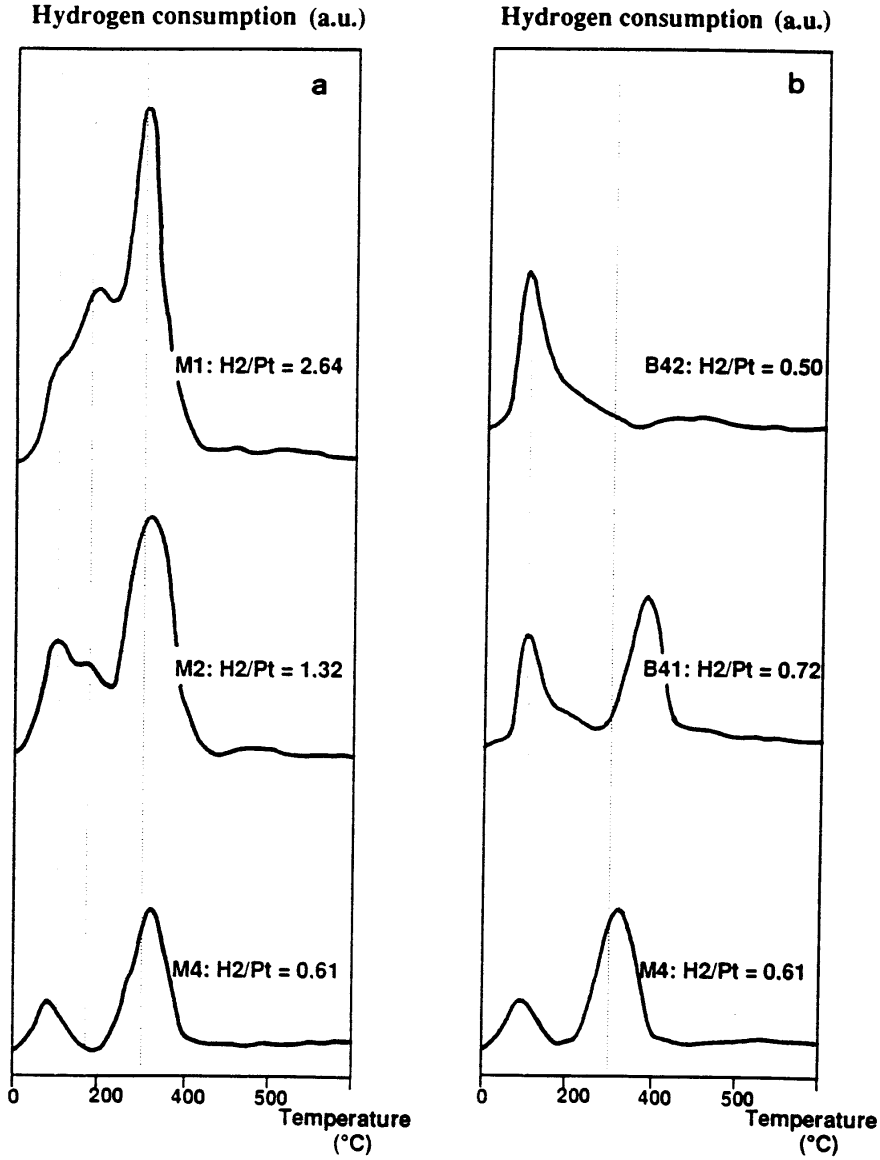

FIG. 7. TPR profiles (a) of monometallic samples M1, M2, and M4 and (b) of samples M4, B42, and B42.

platinum atom per hour) are presented in Table 7. The activity (or TOF) of monometallic catalysts increases with particle size. This may be explained by an electronic effect. If we refer to results previously obtained (33), aromatic cycles with be adsorbed more strongly on the smaller particles, which are electron deficient, than on larger particles and so will poison the catalytic sites. Selectivites of monometallic catalysts for *trans*-dimethylcyclohexane are also listed in Table 7. Selectivity is constant except for the highest dispersion. This may be correlated to a low electron density for small supported metallic particles as is commonly admitted.

As shown in Table 7, bimetallic catalyst activities are much lower than those of corresponding monometallic systems. It is not possible to explain this result by a geometrical effect rather than by an electronic one. Adding tin induces a higher selectivity expect in the case of series 1. As can be seen in the same table, tin has an opposite effect to that of piperidine which is an electron donor compound. This would seem to indicate that the electron density of platinum atoms decreases by adding tin on large particles (series 4). The effect of tin on platinum electron density also depends on the particle size of the catalyst as can be seen in the case of series 1.

4. DISCUSSION

Catalyst Dispersion

The reload technique is able to furnish calibrated average particle sizes. The number of chemisorbed molecules measured by the two techniques of chemisorption used here decreases when the number of steps of loading increases. This corresponds to a decrease in the metal dispersion and is

TABLE 7

TOF Activities Conversion Rates, and Selectivities of Catalysts

Catalysts	wt% Pt	wt% Sn	TOF(h^{-1})	Conversion (%)	Selectivity toward *trans*-DMC6 (%)
M1	0.68		1040	0.76	31.81
M1[a]	0.68		2.5	0.05	17.00
B11	0.69	0.38	226		
B13	0.69	0.82	2.5	0.05	28.30
M2	2.06		1030	8.16	22.88
B21	2.10	1.05	<1		
B22	2.10	1.44	<1	0.02	31.58
M4	3.30		4054[b]	3.16	21.15
M4[a]	3.30		2.4[b]	0.06	16.80
B41	3.26	0.44	383	3.08	33.10
B42	3.28	1.16	5.1	0.24	38.08

[a] Feed + 2 wt% of piperidine.
[b] Measured at 120°C.

confirmed by histograms obtained from TEM results. These are shifted progressively to higher sizes.

When tin is added, the quantity of chemisorbed hydrogen decreases. Larger particle size or a selective deposit of tin on platinum may explain this result. It has been shown by TEM that changes in particle sizes by adding tin depend on the average size of the monometallic precursor. Series 4 is of particular interest. Indeed, no evolution can be seen in histograms of this series. However, the H_2/Pt ratio decreases dramaticaly when tin loading increases. Therefore, it can be concluded that tin is selectively deposited on platinum. Changes of size due to the addition of tin on particles cannot be visualized if the particles are too large. If we assume that a monoatomic layer of tin is deposited on the particles, changes in size will be too small to be detected. Observations made on series 1 and 2 may be discussed in a similar manner. For a highly dispersed metallic phase (M1), numerous particles are probably not visualized because their size is below the detection limit (0.7 nm). When tin is added, growth of these particles could reveal them thus changing the histogram without modifying the size of the dominant population. A shift of the maximum of the histograms is clear only for series 2 and supports the hypothesis of a selective deposit of tin on platinum during catalyst preparation. Finally, results obtained by IR(CO) showing loss of accessibility of Pt by measuring the surface of the ν_{C-O} band at 150°C were coherent with variations in H_2 chemisorption as shown in Table 8.

Surface Composition

LEIS measurements show that the first atomic layer is tin rich whatever the particle size and the Pt/Sn nominal ratio. In addition, this tin enrichment decreases with the depth of analysis for calcined samples. These results confirm the hypothesis which had to be made to explain Pt/Sn ratios

TABLE 8

Comparison of Losses of Platinum Accessibility due to Tin Addition Determined by H_2 Chemisorption and IR

Samples	H_2 chemisorption (%)	IR (%)
B11	40	44
B12	56	44
B21	48	45
B22	63	38
B41	17	16
B43	52	44

obtained by XPS: $(Pt/Sn)_{XPS}$ ratios were always lower than nominal ratios, and only a tin enrichment may explain this fact. Finally, XEDS analyses are in agreement with a surface reaction of tin on platinum. Pt/Sn ratios obtained for both support and particles show a specific reaction of tin with accessible platinum atoms. These ratios are close to 1 for the highly dispersed platinum on the support and increase with the particle size.

Oxidation State

Oxidation states of tin have been determined after calcination and reduction. As already said, it is possible, by XPS, to distinguish metallic and oxide forms of tin but not the two forms of oxidized tin. Metallic tin is present in low proportion in all calcined samples (more than the 15% found for the calcined Sn monometallic sample). Part of the tin is difficult to oxidize and so could be present as an alloy. In contrast, total reduction of the other part of tin is limited in particular for highly dispersed catalysts. The proportion of metallic tin in reduced samples increases with particle size and, for a given particle size, with tin loading. Thus bimetallic phases are more easily obtained for larger particles than for small ones. In this latter case, particles may be too small to stabilize tin in the metallic state. Tin probably migrates onto the support and remains in an oxidized state.

For all samples, both metallic and oxidized tin are detected. Although platinum in Pt–Sn/Al_2O_3 is fully reduced as shown by previous XANES results (31), analysis of hydrogen consumption shows that reduction of bimetallic phases requires less hydrogen than reduction of the corresponding monometallic precursor (Table 6). Part of the platinum probably stays in a metallic state during calcination. The formation of a bimetallic phase could again be envisaged and is coherent with XPS results showing the presence of metallic tin after calcination. For bimetallic catalysts, reduction temperatures are similar to those of platinum oxide in weak interaction with the support. Even though tin cannot be fully reduced to the metallic form and incorporated into an alloy, it modifies the properties of

TABLE 9

Selectivites Toward *trans*-DMC6 and IR Wavenumbers for Monometallic Samples

Samples	Dispersion (%)	Selectivity in *trans*-DMC6 (%)	IR wavenumbers after desorption (cm^{-1})
M1	87	31.81	2033
M2	63	22.88	2037
M3	51	23.01	
M4	32	21.15	2041

platinum particles supported on alumina and seems to play a role of buffer between particles and support.

Electronic Effects

For bimetallic systems, variations in catalytic properties can be used to study electronic modification of the main component due to the addition of a second metal (tin) because adsorption processes of hydrocarbons are modified by this (29). Two techniques have been used in order to gain information on this point: the first is a catalytic reaction (orthoxylene hydrogenation) which is sensitive to electronic effects, and the second is IR coupled with CO chemisorption.

Selectivity to *trans*-dimethylcyclohexane in the xylene hydrogenation reaction is highest for the smallest particles (see Table 9). Thus from catalysis results, the electronic density of surface platinum atoms in monometallic samples seems lowest for the smallest particle size. In contrast, IR results (Table 9) would seem to indicate that the electronic density is higher for the smaller particles. It is difficult to explain this result in contradiction with XANES results (34) showing electron deficiency for small particles.

Concerning bimetallic systems, interpretations of the IR and catalysis results again diverge. For catalytic tests, there is an electronic transfer from Pt to Sn, whereas Pt is not modified by Sn according to IR measurements. In this case, the latter results are in agreement with IR results already published (35). According to another study (21), under the conditions of IR analysis (vacuum, temperature), reduced tin may be reoxidized by protons of the support and be segregated from the platinum particles.

5. CONCLUSION

The aim of this work was to characterize bimetallic Pt–Sn/Al_2O_3 catalysts prepared using organometallic precursors. Evolution of the different phases may be described as a function of treatments applied to catalysts and of the particle size by the scheme presented in Fig. 8.

As already described (18), decomposition of $SnBu_4$ on alumina supported platinum catalysts leads mainly to the formation of a bimetallic phase. Upon calcination, tin is

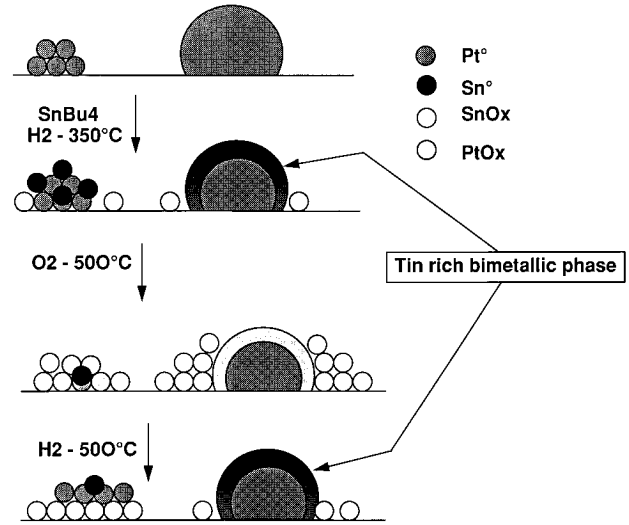

FIG. 8. Schematic representation of different phases depending on particle size.

mostly reoxidized whatever the particle size. Reduction of these systems does not result in the transformation of all of the tin to metallic tin. Considering first the highly dispersed systems, little metallic tin is obtained after this treatment. Properties of the metallic phase are however greatly modified (TPR). This suggests an important interaction between tin oxide and platinum, which could isolate the particles from the alumina. EXAFS experiments previously reported have shown interaction between platinum and oxidized tin in the support through oxygen bonds (31). In the case of low dispersion (particle size >2 nm), a large part of tin is reduced. The proportion of reduced tin increases with tin content. A bimetallic phase is obtained but does not seem to be a stoichiometric alloy as there is segregation of tin at the surface of the particles. For the oxidized tin, the assumption already made for the highly disperse system is still valid. Results of catalytic tests support those obtained by XANES for bimetallic systems.

Two models, depending on average platinum particle size, may thus be proposed in order to describe solids obtained using organometallic precursors:

- A Pt/SnO_x/Al_2O_3 system, in which platinum is probably in interaction with tin oxide, results from a highly dispersed monometallic precursor. For this kind of material, catalyst properties could be due to a strong modification of platinum particle structure rather than to an alloy effect.
- $PtSn^0$/Al_2O_3 bimetallic systems are obtained from large platinum particles. The formation of an alloy-type phase induces electronic modification of platinum in this case.

The bimetallic phases obtained depend on the particle size for a given preparation technique. This may explain discrepancies in the literature concerning these phases. The

particle size has to be taken into account for the study of catalytic properties when adding tin to platinum as the metallic tin to oxided tin ratio is related to this particle size.

ACKNOWLEDGMENTS

We express our thanks to Mr. P. Galguen for preparation of catalysts, to Miss V. Poitrineau for STEM experiments, and to Mr. B. Moisson for IR measurements. Mr. M. de Regt is also acknowledged for his technical contribution.

REFERENCES

1. Li, Y. X., Klabunde, K. J., and Davis, B. H., *J. Catal.* **128**, 1 (1991).
2. Baronetti, G. T., De Miguel, S. R., Scelza, O. A., and Castro, A. A., *Appl. Catal.* **24**, 109 (1986).
3. De Miguel, S. R., Baronetti, G. T., Castro, A. A., and Scelza, O. A., *Appl. Catal.* **45**, 61 (1988).
4. Universal Oil Products Company, U.S. Patent 3,745,112 (1973).
5. Li, Y. X., Zhang, Y. F., and Klabunde, K. J., *Langmuir* **4(2)**, 385 (1988).
6. Li, Y. X., and Klabunde, K. J., *J. Catal.* **126**, 173 (1990).
7. Li, Y. X., and Klabunde, K. J., *Langmuir* **3(4)**, 558 (1987).
8. Margitfalvi, J., Szabó, S., and Nagy, F., *Stud. Surf. Sci. Catal.* **27**, 372 (1983).
9. Bournonville, J. P., and Trinh Dinh, C., U.S. Patent 4549918 (1981).
10. Paffett, M. T., and Windham, R. G., *Surf. Sci.* **208**, 34 (1989).
11. Paffett, M. T., Logan, A. D., Simonson, R. J., and Koel, B. E., *Surf. Sci.* **250**, 123 (1991).
12. Chojnacki, T. P., and Schmidt, L. D., *J. Catal.* **129**, 473 (1991).
13. Pakhomov, N. A., Buyanov, R. A., Moroz, E. M., Yurchenko, E. N., Chernyshev, A. P., Zaitseva, N. A., and Kotelnikov, G. R., *React. Kinet. Catal. Lett.* **14(3)**, 329 (1980).
14. Srinivasan, R., De Angelis, R. J., and Davis, B. H., *J. Catal.* **106**, 449 (1987).
15. Srinivasan, R., Rice, L. A., and Davis, B. H., *J. Catal.* **129**, 257 (1991).
16. Meitzner, G., Via, G. H., Lytle, F. W., Fung, S. C., and Sinfelt, J. H., *J. Phys. Chem.* **92**, 2925 (1988).
17. Muller, A. C., Engelhard, P. A., and Weisang, J. E., *J. Catal.* **56**, 65 (1979).
18. Vértes, Cs., Tálas, E., Czakó-Nagy, I., Ryczkowski, J., Göbölös, S., Vértes, A., and Margitfalvi, J., *J. Appl. Catal.* **68**, 149 (1991).
19. Weishen, Y., Liwu, L., Yining, F., and Jingling, Z., *Catal. Lett.* **12**, 267 (1992).
20. Zhou, Y., and Davis, S. M., *Catal. Lett.* **15**, 51 (1992).
21. Bacaud, R., Bussiere, P., and Figueras, F., *J. Catal.* **69**, 399 (1981).
22. Srinivasan, R., and Davis, B. H., *Appl. Catal.* **82**, 45 (1992).
23. Adkinds, S. R., and Davis, B. H., *J. Catal.* **89**, 371 (1984).
24. Jin, L. Y., *Appl. Catal.* **72**, 33 (1991).
25. Stencel, J. M., Goodman, J., and Davis, B. H., *in* "Proceedings 9th International Congress on Catalysis, Calgary, 1988" (M. J. Phillips and M. Terman, Eds.), p. 1291. Chemical Institute of Canada, Ottawa, 1988.
26. Li, Y. X., Stencel, J. M., and Davis, B. H., *Appl. Catal.* **64**, 71 (1980).
27. Cholley, T., Merlen, E., Le Peltier, F., and Didillon, B., to be published.
28. Atrei, A., Bardi, U., Rovida, G., Torrini, M., Zanazzi, E., and Ross, P. N., *Phys. Rev B* **46(3)**, 1649 (1992).
29. Del Angel, G., Tzompantzi, F., Gomez, R., Baronetti, G., De Miguel, S., Scelza, O., and Castro, A., *React. Kinet. Catal. Lett.* **42(1)**, 67 (1990).
30. Lieske; H., Lietz, G., Spindler, H., and Völter, J., *J. Catal.* **81**, 8 (1983).
31. Caballero, A., Dexpert, H., Didillon, B., Le Peltier, F., Clause, O., and Lynch, J., *J. Phys. Chem.* **97**, 11283 (1993).
32. Aramendia, M. A., Borau, V., Jiménez, C., Marinas, J. M., Rodero, F., and Sempere, M. E., *React. Kinet. Catal.* **46(2)**, 305 (1992).
33. Boitiaux, J. P., Cosyns, J., and Vasudevan, S., *Stud. Surf. Sci. Catal.* **16**, 123 (1982).
34. Yoshitahe, H., and Iwasaw, Y., *J. Phys. Chem.* **95**, 7368 (1991).
35. Balakrishnan, K., and Schwank, J., *J. Catal.* **138**, 491 (1992).